

PROCEEDINGS OF SPIE

SPIDigitalLibrary.org/conference-proceedings-of-spie

In search of a sharper line focus: rotating the étendue

Håkon J. D. Johnsen, Juan C. Miñano

Håkon J. D. Johnsen, Juan C. Miñano, "In search of a sharper line focus: rotating the étendue," Proc. SPIE 12220, Nonimaging Optics: Efficient Design for Illumination and Solar Concentration XVIII, 1222006 (3 October 2022); doi: 10.1117/12.2633358

SPIE.

Event: SPIE Optical Engineering + Applications, 2022, San Diego, California, United States

In search of a sharper line focus: Rotating the étendue

Håkon J. D. Johnsen^{*a} and Juan C. Miñano^b

^aDepartment of Mechanical and Industrial Engineering, Norwegian University of Science and Technology, Trondheim, Norway

^bCedint, Universidad Politécnica Madrid, Spain

ABSTRACT

Conventional line-focus solar concentrators are limited by the 2D concentration limit, two orders of magnitude lower than the three-dimensional limit. This leads to low concentration ratios and strict manufacturing tolerances. It has been shown that by eliminating the continuous translational symmetry of these systems, it is possible to go beyond the 2D limit while maintaining the linear geometry of a line focus. We demonstrate that one way to break this symmetry is through étendue rotation, and we present two new concentrator configurations based on this insight. The first configuration uses an étendue rotating retroreflector array to boost the concentration of a parabolic trough. Ray-tracing simulations show that this configuration can achieve very high geometric concentration ratios or very high acceptance angles (1484x at ± 9 mrad acceptance angle, or 25x at ± 70 mrad). However, this configuration requires two-axis external solar tracking. To get around this, we demonstrate a second configuration that uses an étendue rotating lens array with tracking integration. We demonstrate a design that achieves a geometric concentration of 146x at a ± 9 mrad, with a simulated average yearly efficiency of 94.9% when used with conventional horizontal single-axis external tracking at an installation latitude of 30° . The extra constraints of the tracking integration gives this design a more modest concentration ratio, but it is still higher than the 2D concentration limit and more than three times as high as the concentration of a parabolic trough evaluated under the same conditions. We believe that these new configurations show that the design landscape for line-focus solar concentrators can be widened, and that a practical high-concentration line-focus concentrator may be within reach.

Keywords: solar concentration, étendue rotation, étendue squeezing, parabolic trough, tracking integration, concentrated solar power

1. INTRODUCTION

The thermodynamic three-dimensional concentration limit for solar concentrators is well established, giving a fundamental limit for the concentration of any solar concentrator.¹ For concentration in air, it is given by Eq. 1:

$$C_{max,3D} = \frac{1}{(\sin \theta)^2}, \quad (1)$$

where θ is the acceptance angle of the optics, and must be large enough for the approximately 4.7 mrad angular radius of the sun convolved with the effect of manufacturing tolerances. Assuming an acceptance angle of $\theta = 9$ mrad, the concentration limit becomes $C_{max,3D,9\text{ mrad}} = 12\,346$.

There is a corresponding and much lower concentration limit, given by Eq. 2, that applies to two-dimensional systems:

$$C_{max,2D} = \frac{1}{\sin \theta} \quad (2)$$

Under the same acceptance angle $\theta = 9$ mrad, this becomes $C_{max,2D,9\text{ mrad}} = 111$. The two-dimensional limit applies to traditional line-focus concentrators such as parabolic troughs and linear Fresnel collectors, because these are essentially two-dimensional concentrators extruded in the third dimension.¹ As a result, the concentration ratio of line-focus concentrators is orders of magnitude lower than that of solar towers and parabolic dishes.²

* E-mail: hakon.j.d.johnsen@ntnu.no

It has previously been shown that it is possible to concentrate sunlight to a continuous line-focus at concentrations greater than the 2D limit if the continuous linear symmetry of the concentrator is broken.³⁻⁶ In previous research, we have demonstrated that one way to perform this symmetry-breaking is through étendue squeezing.^{7,8}

An alternate and lesser known principle for breaking the continuous translational symmetry of an optical system is étendue rotation.⁹ Here, we show through two different configurations how this principle can be used to increase the concentration of line-focus solar concentrators beyond the 2D concentration limit.

2. ÉTENDUE ROTATORS

Étendue rotation is an approach for rotating the angular extent of a ray bundle. It is especially useful for manipulating ray bundles that have a wide angular extent along one axis and a smaller angular extent along another axis. A rigorous introduction to étendue rotation is given by Benítez et al.⁹ Here, we content ourselves with a simple introduction to the principle, focusing on demonstrating two configurations that can be applied to solar concentrators.

2.1 Étendue rotating retroreflector array

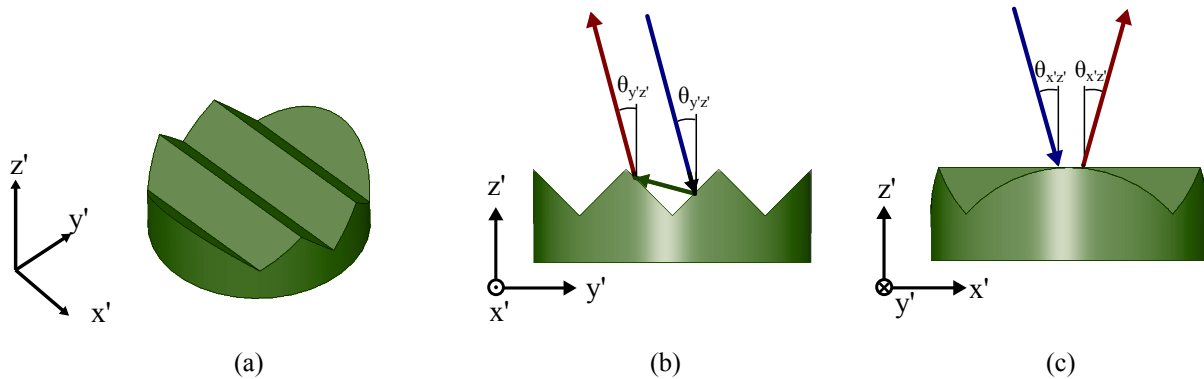


Figure 1. (a) Simple linear retroreflector array in a local coordinate system where the x' -axis points along the retroreflector ridges. (b) In the projection onto the $y'z'$ -plane, incoming rays are retroreflected. (c) In the projection onto the $x'z'$ -plane, incoming rays are reflected normally.

A linear two-dimensional retroreflector (Fig. 1a) can be used to construct an étendue rotator. To illustrate this effect, consider how the behavior of the retroreflector depends on the point of view: When viewed across the retroreflector ridges (Fig. 1b), the device performs retroreflection — rays are reflected back towards their source. However, when viewed along the ridges, the rays undergo regular reflection (Fig. 1c).

The behavior of the linear retroreflector can be illustrated in direction cosine space as shown in Fig. 2a. Retroreflection in the $y'z'$ -plane gives rise to a flipped sign of the q' component, while regular reflection in the $x'z'$ -plane leads to a conserved p' component. The same effect applies to extended ray bundles, and leads to a mirroring of direction cosine across the p' axis as shown in Fig. 2b. Suppose we rotate the retroreflector 45 degrees compared to the global coordinate system. In that case, we get the behavior shown in Fig. 2c. The result is a reflector that can take a ray bundle with a large angular extent in the yz -plane (wide range of q -components in direction cosine space), and convert it into a ray bundle with a large angular extent in the xz -plane. This behavior is further illustrated in the ray trace shown in Fig. 2d, where a set of rays with an angular extent of $\pm 25^\circ$ in the yz -plane is reflected off the retroreflector array. After retroreflection, the angular extent has been rotated, so that the ray bundle now has a large large angular extent in the xz -plane.

The resulting effect of transferring the angular extent from one plane into another is known as étendue rotation, and was first introduced by Benítez et al.¹⁰

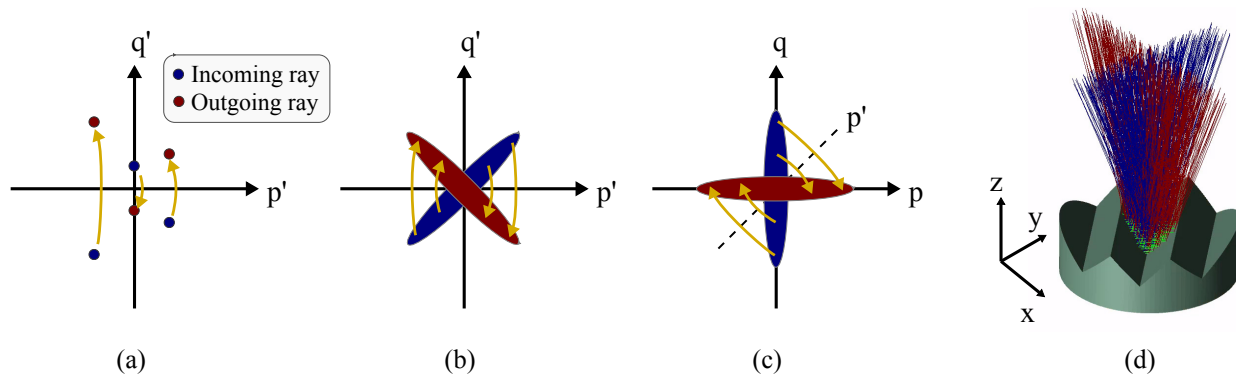


Figure 2. (a) In direction cosine space, the retroreflector flips the sign of the q' component of a ray while leaving the p' component unchanged. Here, p' is direction cosine along the local x' -axis, and q' is direction cosine along the local y' -axis. (b) The same effect applies to extended ray bundles. (c) When drawn in a global coordinate system rotated 45° , angular extent can be exchanged between different axes, giving rise to étendue rotation. (d) A bundle of rays with wide angular extent in the xz -plane is converted to a bundle of rays with a large angular extent in the xz -plane upon retroreflection.

2.2 Étendue rotating lens arrays

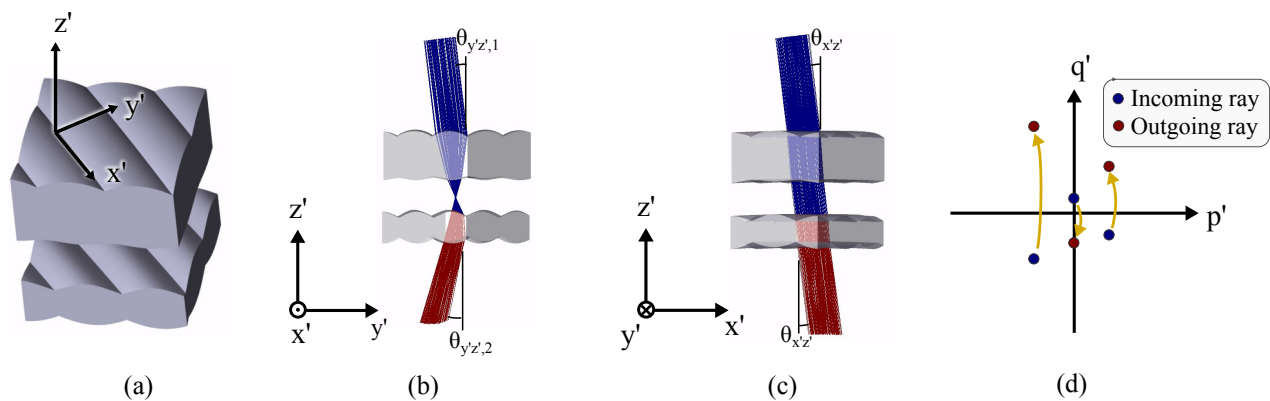


Figure 3. (a) A pair of cylindrical lens arrays use to demonstrate étendue rotation. (b) In the $y'z'$ -plane, these lens arrays form a Keplerian telescope, giving a negative angular magnification. (c) In the $x'z'$ -plane, the lens arrays don't affect the angle of incoming rays. (d) In direction cosine space, the q' -components therefore receive a negative magnification, while the p' -components remain unchanged.

Étendue rotation can also be implemented using cylindrical lenses. Benítez et al.⁹ derived the concept using a paraxial afocal cylindrical lens pair. Here we demonstrate the principle using a pair of cylindrical lenses in a configuration that will be better suited for solar concentration.

Consider the pair of cylindrical lenses shown in Fig. 3a with a local coordinate system $x'y'z'$. In the $y'z'$ -plane, these lenses form an approximately afocal optical system with a negative angular magnification, as shown in Fig. 3b. In the $x'z'$ -plane, on the other hand, the lenses do not affect the angle of the rays as shown in Fig. 3c. In direction cosine space, this behavior can be illustrated as shown in Fig. 3d. The behavior is similar to the one shown previously for the retroreflector, except that the magnification of p' -components is not necessarily exactly negative one.

The behavior for an extended ray bundle is shown in Fig. 4a. By rotating the lens array compared to the global coordinate system xyz , the étendue rotating effect is achieved. However, to compensate for the angular magnification in the $y'z'$ -plane not being exactly equal to negative one, the required rotation angle is no longer exactly 45° .

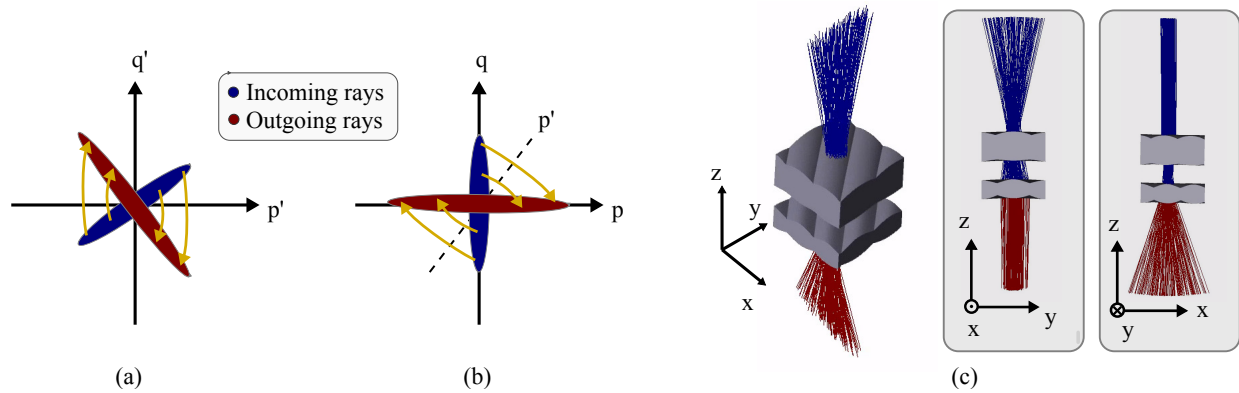


Figure 4. (a) Behavior of the lens array from Fig. 3, schematically drawn in the local direction cosine space. p' is direction cosine along the x' -axis, and q' is direction cosine along the y' -axis. (b) In the global coordinate system, the lens arrays perform étendue rotation. (c) Ray-traced model of the lens array, showing the lenses performing étendue rotation. Incoming light with a wide angular extent in the yz -plane is converted to light with a wide angular extent in the xz -plane.

2.3 Tracking-integration

The étendue rotator made from a pair of cylindrical lens arrays can be designed to gain an important extra functionality: Tracking integration. In this way, the lens array is able to maintain its étendue rotation effect while handling a nonzero angle of incidence.

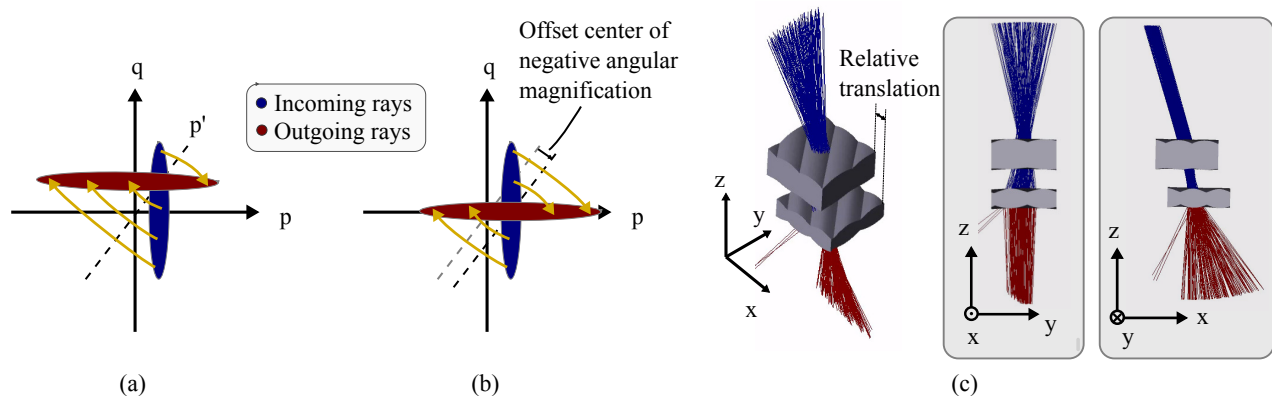


Figure 5. (a) With a nonzero angle of incidence in the xz -plane (nonzero p component in direction cosine space), the outgoing rays get a corresponding nonzero angle in the yz -plane after étendue rotation. (b) Tracking integration can compensate for this effect, so that the outgoing rays again have an angle close to zero. (c) Ray-traced illustration of this principle. With the help of a relative translation between the two lens arrays, the lenses are still able to remove the angular extent from the yz -plane.

Consider an incoming ray-bundle with a non-zero angle of incidence in the xz -plane. Fig. 5 shows how the étendue rotator converts this into a ray-bundle with a non-zero angle in the yz -plane. However, if the two lens arrays are moved relative to each other, it is possible to change their behavior, and recover the behavior where the outgoing rays have an angle close to zero in the yz -plane. This effect is illustrated in Fig. 5b, and a ray-traced demonstration of the effect is shown in Fig. 5c. This capability to handle a non-zero angle of incidence becomes important when using the étendue rotator in a solar concentrator.

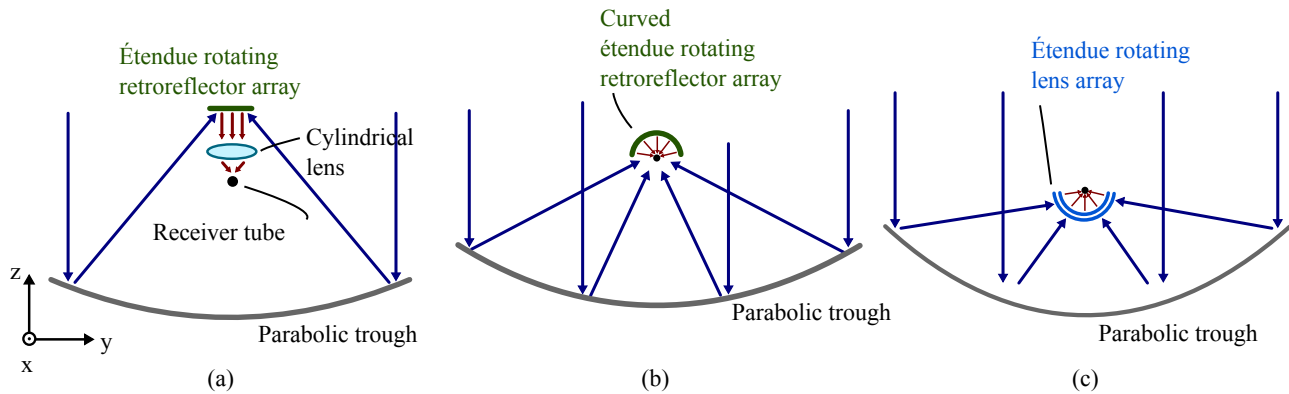


Figure 6. (a) A parabolic trough utilizing étendue rotation to increase linear concentration. A similar configuration was first proposed by Davidson et al.⁶ (b) By curving the retroreflector array around the receiver, the component number can be reduced and the rim angle of the parabolic trough can be increased. (c) Using a pair of étendue rotating lenses instead of retroreflectors makes it possible to increase the rim angle further and makes it possible to support tracking integration.

3. ÉTENDUE ROTATION IN LINEAR SOLAR CONCENTRATORS

Sunlight concentrated by a linear concentrator has a wide angular extent in the transverse plane (the yz -plane in Fig. 6) due to étendue conservation in this plane. However, the angular extent in the longitudinal plane (the xz -plane) remains low due to the low angular extent of direct sunlight. This makes it possible to use an étendue rotator to dump the high angular extent from the transverse plane into the longitudinal plane, allowing a further concentration step in the transverse plane. In this way, the sunlight can be concentrated onto a smaller tubular receiver as conceptually illustrated in Fig. 6a. The idea of using a retroreflector in this configuration was, to our knowledge, first proposed by Davidson et al.,⁶ albeit using somewhat different terminology. In Figs. 6b-c we propose two new étendue rotator configurations for linear solar concentration that we explore further in the remainder of this paper.

3.1 Linear solar concentrator with étendue rotating retroreflector array

By curving the retroreflector array so that its surface normal always points toward the receiver tube, the extra cylindrical lens from Fig. 6a can be eliminated, giving the configuration shown in Fig. 6b.¹¹ At each local point of the curved retroreflector, it accepts a bundle of rays with a large angular extent in the transverse (yz) plane and converts it into a bundle approximately parallel to the surface normal. Since the surface normal points toward the receiver tube, this directly performs the secondary concentration step without requiring an extra secondary concentrator.

We created two different example designs using this principle. One concentrator was designed to achieve conventional concentration ratios under a very high acceptance angle. Zemax OpticStudio simulations show that under sunlight with a top-hat angular distribution of $\pm 4^\circ$ (± 70 mrad), this concentrator achieved a simulated optical efficiency of $\eta = 91.2\%$ at a geometric concentration of $C_g = 25.6$. A ray-traced model of the concentrator is shown in Figs. 7a-b. Fig. 7c shows how the curved retroreflector geometry is implemented, using an array of metallized retroreflector prisms placed diagonally at 45° along the surface of a thin PMMA sheet. This sheet is then curved so that its surface normal always points toward the receiver tube.

The second concentrator was designed for high concentration under stricter tracking requirements, using a smaller étendue rotating retroreflector and a much smaller receiver tube. Under simulated sunlight with a top-hat angular distribution of $\pm 0.52^\circ$ (± 9 mrad), it achieved an efficiency of $\eta = 89.2\%$ with a geometric concentration of $C_g = 1484$. A ray-traced model of the concentrator is shown in Fig. 8 and the design parameters and simulation results for both concentrators are summarized in Table 1.

These examples demonstrate very high concentration ratios or very high acceptance angles compared to conventional linear concentrators, but they require two-axis solar tracking. Conventional linear concentrators usually only use horizontal single-axis tracking, which can be implemented with significantly less mechanical complexity.

Such single-axis tracking is difficult to achieve in this proposed configuration, motivating the development of an alternative configuration based on étendue rotating lens arrays.

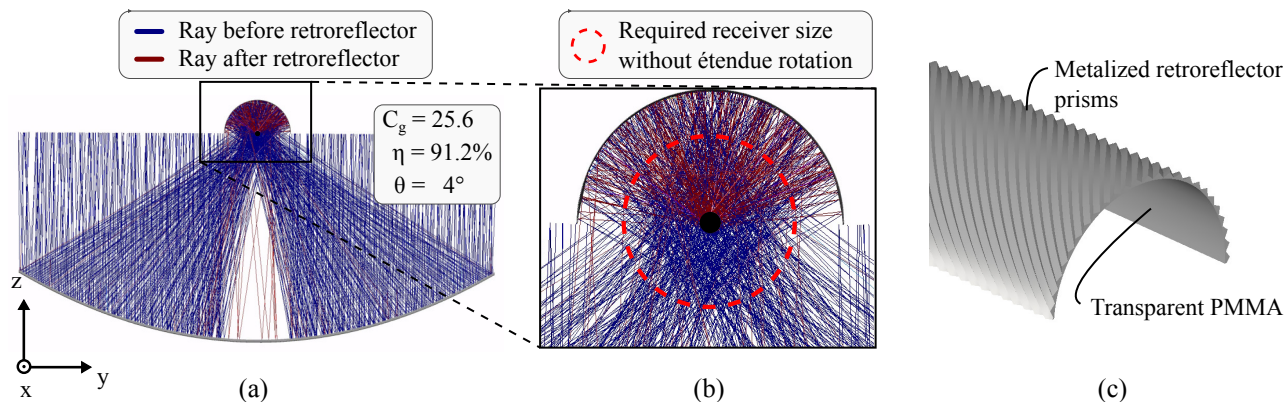


Figure 7. (a) Concentrator for high acceptance angle, ray-traced in Zemax OpticStudio. (b) Close-up of the étendue rotating retroreflector. (c) Schematic 3D model of retroreflector geometry, showing how the retroreflector prisms are made in the surface of a transparent material. By performing the retroreflection inside of a material with $n \approx 1.5$, the angles of incidence are smaller, leading to smaller shading losses in the retroreflector prisms. In the simulation model, the individual prisms in the surface are much smaller than what is shown in this visualization model.

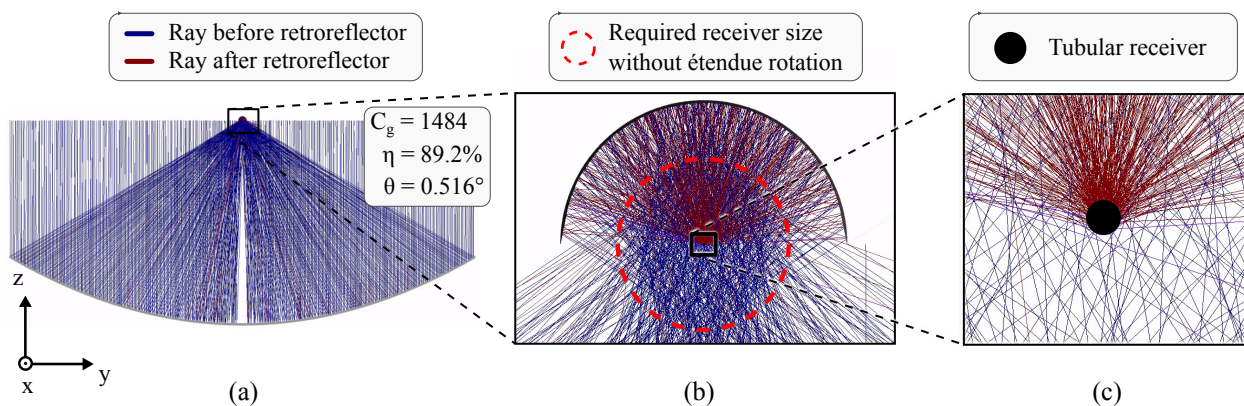


Figure 8. Ray-traced model of concentrator designed for high concentration ratio.

Table 1. Parameters for étendue rotating retroreflector design examples. For simplicity, simulations assume ideal surfaces, ideal reflectors, and no absorption (except at the receiver tube).

Parameter	High concentration	High acceptance angle
Parabola width	1000 mm	1000 mm
Retroreflector diameter	18.0 mm	139.4 mm
Receiver diameter	0.210 mm	10.7 mm
C_g	1484	25.6
Acceptance half-angle	9 mrad (0.52°)	70 mrad (4.0°)
Simulated efficiency	89.2%	91.2%
Tracking requirements	Two-axis	Two-axis

3.2 Linear solar concentrator with étendue rotating lens array and tracking integration

The configuration proposed in Fig. 6c makes it possible to use étendue rotation in a concentrator while maintaining compatibility with horizontal single-axis tracking. This configuration can compensate for a varying longitudinal angle of incidence using tracking integration in the form of relative translation between the two lens arrays. Fig. 9a shows how such a configuration can perform ordinary horizontal single-axis tracking, while Fig. 9b shows the use of tracking integration.

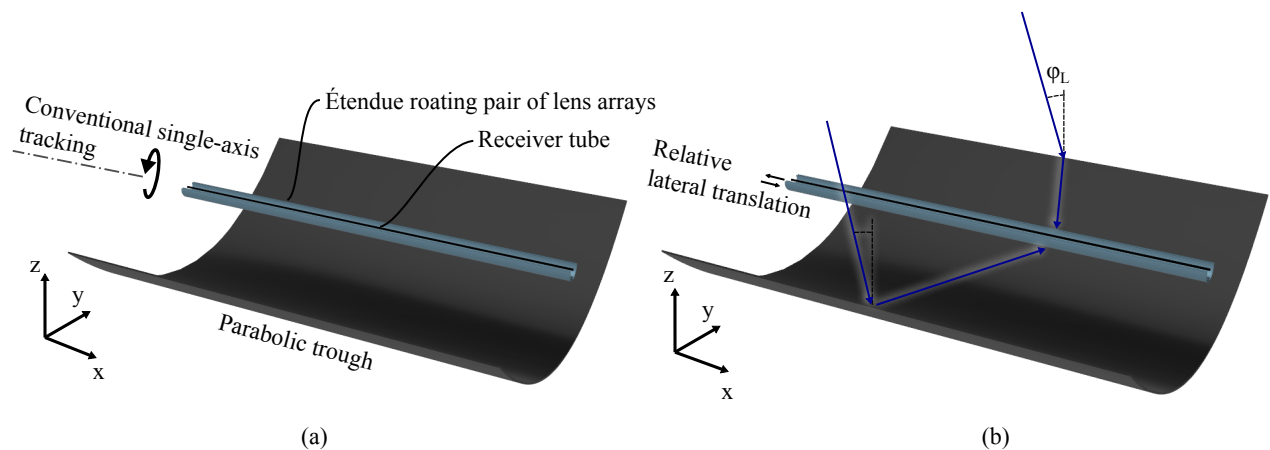


Figure 9. (a) A parabolic trough with an étendue rotating lens array can use conventional horizontal single-axis tracking. (b) A non-zero angle of incidence in the longitudinal plane (xz-plane) is handled through tracking integration, using relative translation between the two lens arrays.

We used ray-tracing and numerical optimization to design an example concentrator utilizing an étendue rotating lens array based on this principle. The system was designed for combination with a parabolic trough, assuming horizontal single-axis solar tracking and an installation latitude of 30°. We used a PMMA material model for the lenses and an AM1.5D spectrum, with room for manufacturing errors through a solar half-angle of 9 mrad and a uniformly distributed slope error on the lenses of ± 8 mrad. Reflection and volumetric absorption losses were not included in this initial model. The optimization was done on computing resources provided by the NTNU IDUN/EPIC computing cluster¹² and the resulting concentrators were simulated in Zemax OpticStudio.

The parameters of the optimized design example is summarized in Table 2, and Fig. 10 shows a ray-traced model of the optimized concentrator. It achieves a simulated average yearly optical efficiency of 94.9% at a geometric concentration of 146x. For comparison, the 2D limit is 111x under the simulated conditions, and a

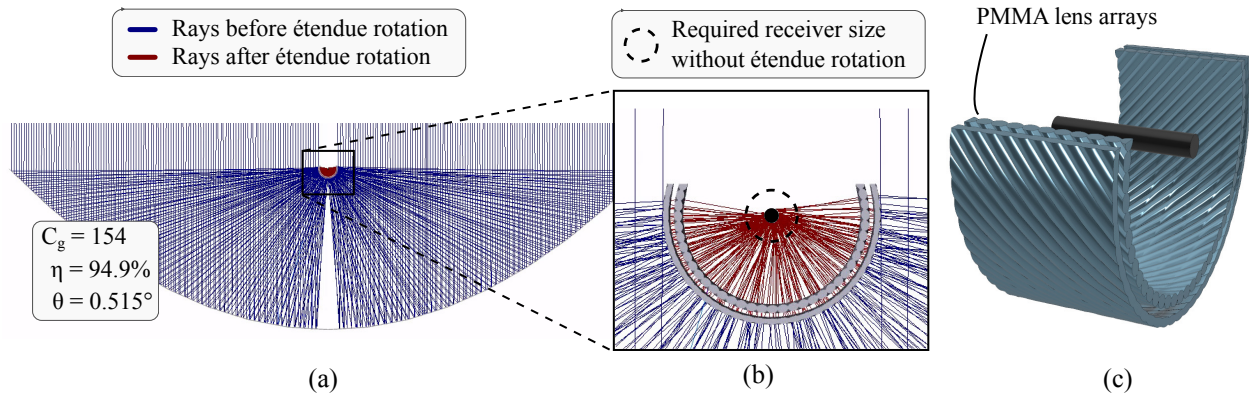


Figure 10. (a) Parabolic trough with étendue rotating lens arrays simulated in Zemax OpticStudio. (b) Close-up of ray-trace showing how the lens arrays redirect the rays to be pointed directly toward the receiver, reducing the required receiver size. (c) 3D model of a section of the étendue rotating lens arrays, showing how they consists of cylindrical lenses following a helical path around the receiver.

conventional parabolic trough reaches 49x if evaluated under the same conditions. Simulated optical efficiency across different longitudinal angles of incidence is shown in Fig. 11

Table 2. Parameters for the étendue rotating lens array design example. For simplicity, simulations assume ideal surfaces, ideal reflectors, and no absorption (except at the receiver tube), but the lens surfaces have been given a uniformly distributed slope error to demonstrate the low sensitivity to such errors.

Parameter	Value
Parabola width	1000 mm
Lens array diameter	31.2 mm
Receiver diameter	2.12 mm
C_g	146
Lens array slope error	Uniformly distributed, ± 8 mrad
Acceptance half-angle	9 mrad (0.52°)
Simulated average yearly efficiency	94.9%
Tracking requirements	Horizontal single-axis external tracking at a simulated 30° latitude

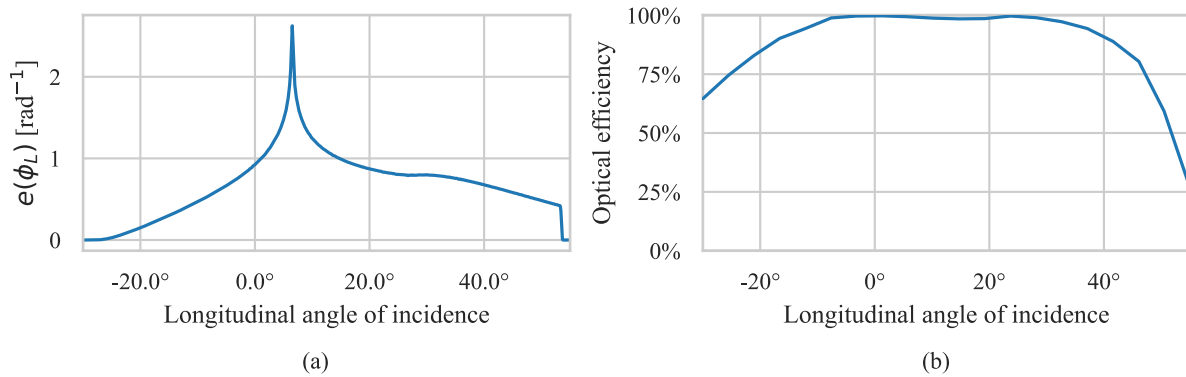


Figure 11. (a) Simulated normalized distribution of the angle of incidence in the longitudinal plane, as seen by a concentrator mounted on a horizontal single-axis external tracker at a latitude of 30°. This gives the tracking range required by the tracking integration to achieve good full-year performance. (b) Simulated efficiency of the example concentrator as a function of angle of incidence, simulated using ray-tracing in Zemax OpticStudio. Integrated over a whole year with the angular distribution from a, gives an average yearly efficiency of 94.9%.

4. OUTLOOK AND CONCLUSIONS

We have shown through optical simulation how étendue rotation can be used to boost the achievable concentration of linear concentrators, reaching values beyond the two-dimensional concentration limit that traditionally governs such systems. We have proposed how the étendue rotator can be curved around the receiver tube, directly performing both étendue rotation and a secondary concentration step enabled by this étendue rotation.

Using a retroreflector as the étendue rotator, we achieved concentration ratios more than an order of magnitude beyond the 2D concentration limit, or alternatively very high acceptance angles at conventional concentration ratios. The design of the retroreflector geometry is straightforward, and does not depend upon numerical optimization. However, the resulting concentrators require two-axis solar tracking, adding additional complexity to such a concentrator.

We showed that the need for two-axis external solar tracking could be eliminated by using a pair of lens arrays as the étendue rotating element. This also enabled using conventional parabolic trough geometry with high rim angles. These lens arrays were optimized assuming relatively large slope errors, demonstrating the ability of this type of optics to perform even if manufactured with wide tolerances.

Étendue rotation can be implemented as a secondary concentration step in conventional parabolic trough collectors or in linear Fresnel collectors. Increasing the concentration ratio of linear concentrators may become suitable for new high-temperature heat-transfer fluids previously only available to solar tower. Alternatively, it may allow for relaxed manufacturing tolerances in linear concentrators while maintaining today's concentration levels. We believe this can broaden the design landscape for line-focus solar concentrators and challenge the conventional concentration trade-offs between line-focus and point-focus systems.

REFERENCES

- [1] Winston, R., Minano, J. C., Benitez, P. G., contributions by Narkis Shatz and John C. Bortz, W., and Bortz, J. C., [*Nonimaging Optics*], Elsevier Science (2005).
- [2] Lovegrove, K. and Stein, W., [*Concentrating Solar Power Technology: Principles, Developments, and Applications*], Woodhead Publishing Series in Energy, Woodhead Publishing (2021).
- [3] Rönnelid, M. and Karlsson, B., "Optical acceptance function of modified compound parabolic concentrators with linear corrugated reflectors," *Applied Optics* **37**(22), 5222–5226 (1998).
- [4] Bortz, J. C., Shatz, N. E., and Winston, R., "Performance limitations of translationally symmetric non-imaging devices," *Proc. SPIE* **4446**, 201–220 (2001).

- [5] Nilsson, J., Leutz, R., and Karlsson, B., “Micro-structured reflector surfaces for a stationary asymmetric parabolic solar concentrator,” *Solar Energy Materials and Solar Cells* **91**(6), 525–533 (2007).
- [6] Davidson, N., Khaykovich, L., and Hasman, E., “Anamorphic concentration of solar radiation beyond the one-dimensional thermodynamic limit,” *Applied Optics* **39**(22), 3963–3967 (2000).
- [7] Johnsen, H. J. D., Aksnes, A., and Torgersen, J., “Beyond the 2D limit: étendue-squeezing line-focus solar concentrators,” *Optics Letters* **46**(1), 42–45 (2021).
- [8] Johnsen, H. J. D., Miñano, J. C., and Torgersen, J., “Line-focus solar concentration 10 times higher than the 2D thermodynamic limit,” *Optics Express* **30**(14), 24362–24374 (2022).
- [9] Benítez, P., Miñano, J. C., and Blen, J., “Squeezing the Étendue,” in [*Illumination Engineering*], 71–99, John Wiley & Sons, Ltd (2013).
- [10] Benítez, P., Miñano, J., Blen, J., and Garcia, F., “étendue squeezing optics: Beating the angle-space compromise of symmetrical systems,” in [*International Nonimaging Optics Workshop*], (2005).
- [11] Johnsen, H. J. D., “Étendue-Rotating Optical Systems.” United Kingdom Patent Application No. 2208530.2 (2022).
- [12] Sjölander, M., Jahre, M., Tufte, G., and Reissmann, N., “EPIC: An Energy-Efficient, High-Performance GPGPU Computing Research Infrastructure,” *arXiv:1912.05848 [cs]* (2021).